Microstructures Formed by Spray Freezing of Food Fats

C.G. Gwie, R.J. Griffiths, D.T. Cooney, M.L. Johns, and D.I. Wilson*

Department of Chemical Engineering, New Museums Site, Cambridge, CB2 3RA, United Kingdom

ABSTRACT: The spray-freezing of two food fats, tripalmitin (PPP) and cocoa butter (CB) and mixtures thereof, has been modeled experimentally using a novel single droplet freezing apparatus configured so that temperature profiles or samples for microstructure analysis can be obtained. For 2 mm diameter droplets suspended in a cold air flow at temperatures around 2–15°C, initial cooling rates were on the order of 10 K s^{-1} and the temperature profiles could be correlated directly to DSC data collected at 20 K min^{-1}, indicating that minimal supercooling of the materials occurred in the droplet form. Microstructure analysis confirmed that PPP crystallized preferentially in mixtures, and that the surface structure was very sensitive to storage conditions. The bulk structure was much less sensitive, and the internal microstructure of the PPP droplets revealed distinct nucleation sites, which were absent from the CB: These persisted in the mixtures up to 50 wt%. X-ray analysis indicated that the fats crystallized in their more stable forms, namely, β for PPP and Form V/VI in CB.

Paper no. J11252 in *JAOCS 83*, 1053–1062 (December 2006).

KEY WORDS: Cocoa butter, microstructure, polymorphs, spray freezing, tripalmitin.

Spray freezing of liquids and emulsions by exposing fine drops to cold, dry gas (usually air) has been advocated as a manufacturing route for new products and product forms by several workers (e.g., 1–3). This route allows thermally labile products to be converted to the form of a free-flowing powder, avoiding structure and activity modification associated with the temperatures required for spray-drying. It offers very high cooling rates, both *via* large surface area-to-volume ratios and high rates of convective heat and mass transfer (i.e., where volatiles give rise to evaporative cooling) and, when operated correctly, yields a fine particulate product with well-defined size range. For aqueous systems, a subsequent freeze-drying step is required to give a stable product. Commercial processes based on this technology are available (see Ref. 2), particularly for spray-chilling for microencapsulation. A number of patents have been filed recently on a variant where the feedstock is contacted with a cryogen spray, typically liquid nitrogen, to give extremely high cooling rates (4–6). Spray-freezing also offers the opportunity to generate new microstructural forms, or direct routes to known forms, driven by the high rate of cooling achievable in drops compared with bulk liquid.

Spray-freezing into liquid has received considerable attention in the pharmaceutical and other controlled release sectors as a way of generating novel microstructures and microencapsulates and for stabilizing enzymes. Interest in the food sector is relatively recent, partly because of the cost associated with the cooling media: spray-freezing into cold air avoids the need to separate the product solids from liquid, which in addition would have to be food grade and noncontaminating. Hindmarsh and co-workers have shown that spray-freezing in air or cold nitrogen gas can yield novel structures from sucrose solutions (7) and emulsions (8), and MacLeod *et al*. (9) have demonstrated that spray-freezing followed by freeze-drying of coffee solutions can yield powders with much finer microstructure than achieved by traditional routes.

There is considerable interest in the food sector in the spray freezing of fats (e.g., 5), for example, as a way of generating free-flowing powders that can be readily mixed into doughs and of reducing the loading required to achieve dough consistency for low-fat formulations. Freezing of mixtures of fats offers possibilities of controlling microstructure *via* phase separation, whereby differences in m.p. can result in preferential crystallization of one species. Furthermore, many food fats exhibit polymorphism, which is sensitive to cooling rate. The crystalline state of lipids has been reviewed by Lutton (10). Spray-freezing of fats to yield powders with a preferred polymorphic form, e.g., the form V preferred in cocoa butter, could then be exploited in cold processing for shaped products. This paper describes an initial investigation of microstructures generated in simulated spray-freezing of mixtures of cocoa butter and tripalmitin (PPP).

Spray-freezing was studied in a single-droplet freezing apparatus based on that reported by Hindmarsh *et al*. (7). Individual droplets are frozen in a cold air stream while suspended on a fine thermocouple or a glass filament. The former allows the thermal history of the droplet to be monitored directly, as the droplet temperature is almost uniform (low Biot number: see Ref. 9), whereas the latter yields droplets that can be analyzed readily. Microstructures were studied by scanning electron microscopy (SEM) and by small- and wide-angle X-ray scattering (SAXS and WAXS, respectively); the 1–2 mm frozen droplets generated here were almost an ideal geometry for X-ray scattering measurements.

MATERIALS AND METHODS

Materials. Cocoa butter (Gerkens Cacao, B.V., Wormer, The Netherlands) and PPP (85% purity; Sigma Chemical, Poole, United Kingdom) were obtained as solids and studied as pure

*To whom correspondence should be addressed at Dept. of Chem. Engineering, New Museums Site, Pembroke St., Cambridge CB2 3RA, United Kingdom. E-mail: diw11@cam.ac.uk

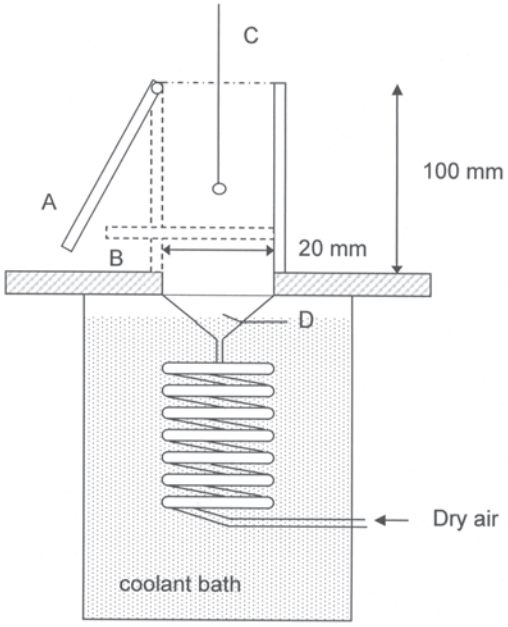

FIG. 1. Single droplet freezing apparatus. (A) Pivoted side wall which allows gate (B) to divert cold air flow while a droplet is located on the end of a thermocouple measuring T_d (droplet temperature) or filament (as shown) at C. Cooling air temperature, T_a, measured by thermocouple at D.

components and as mixtures of 25, 50, and 75 wt% PPP in cocoa butter. Mixtures were obtained by melting the components together and mixing vigorously. Phase transitions in the raw materials and mixtures were studied on a PerkinElmer Pyris 1 power-compensated DSC (PerkinElmer Life & Analytical Sciences Inc., Boston, MA) fitted with a refrigerated intercooler. Samples were heated in sealed pans to 80°C then cooled to –20°C (100 to 0°C for PPP alone) at 20 K min^{-1}. This cycle was performed three times using the same sample, and repeated twice, using new samples to establish reproducibility.

Droplet freezing. Freezing of individual droplets was studied in the apparatus shown in Figure 1. A detailed description is given in Reference 9. Laboratory compressed air at 1 bar was passed through a silica-gel dehumidifier, a rotameter, and a copper coil immersed in a glycol/water cooling bath mounted on a Haake K20 refrigerated cooler (Thermo Electron Corp., Basingstoke, United Kingdom) to give cold, dry air at the required temperature T_a. The air then passed through a vertical, square-sided duct of width 20 mm and length 100 mm fabricated from Perspex, open to the atmosphere. A thin (50 μm) T-type thermocouple or a glass filament (diameter 50–200 μm) was located on the centerline of the duct, 30 mm from the open end (9). Droplets were suspended from the end of the thermocouple or filament, which was coated with nail varnish to help the droplet adhere without promoting nucleation (8). A second thermocouple located at the duct entry measured T_a. Both thermocouples were calibrated regularly against the freezing point of water: T_a and droplet temperature, T_d, were both monitored and recorded on a PC.

Each sample was heated to a temperature well above its m.p. to eradicate crystallization history and avoid solidification while preparing droplets. For the 2 mm diameter droplets studied here, 8 μL was measured out and suspended using a prewarmed Hamilton 701 LT 10 μL syringe, which was kept warm at 80°C, making use of the gate construction to divert the "cold" air flow while positioning the droplet. For repeated runs, a hand-held hair dryer was used to remelt solidified droplets or further heat the suspended droplet to the required temperature range (in excess of 70°C), holding T_d constant for at least 20 s. Reheating was not used in the generation of droplets for X-ray analysis. Droplet size and shape were measured using an Intel® Play (Santa Clara, CA) microscope.

Air flow rates of 0.6 and 1.2 $m^3\ h^{-1}$ were used, corresponding to superficial velocity, u_m, values of 0.42 and 0.83 m s^{-1}. These values correspond to duct (and particle) Reynolds numbers at T_a = 10°C of 600 (120) and 1,200 (240), respectively; separate hot wire anemometry measurements of gas velocity indicated that the local velocity upstream of the droplets approached 2 u_m. These velocities are lower than the terminal velocities for single droplets under these conditions but are representative of those likely to be experienced in a swarm. Droplets for microstructural analysis were mainly generated using a u_m value of 0.42 m s^{-1}. The apparatus was cleaned between runs using hot dodecane and cold acetone.

Droplet microstructure. Frozen droplets were slice-sectioned to expose the internal microstructure, coated with Au/Pd (70%/30%) and then imaged on a Philips XL30-FEG cryo-scanning electron microscope (CSEM) operating at 5 kV.

X-ray diffraction (XRD) studies were performed using a customized Bruker GADDS system, using a Cu source (λ = 1.541 Å) at 45 kV and 45 mA. For WAXS, the detector was positioned 0.174 m from the sample, at an angle of 14° off the centerline. Exposures were performed at room temperature for a maximum of 150 s or 5×10^6 counts. In this period the droplet did not change appearance visibly. For SAXS, the detector was placed on the centerline at 0.782 m from the sample and a Perspex tube containing helium placed between the sample and the detector. Exposures were limited to 60 s. For simultaneous WAXS/SAXS, the detector was placed at 0.174 m/9.2° and exposures set to the shorter of 100 s or 5×10^6 counts.

RESULTS AND DISCUSSION

Freezing behavior. DSC. DSC studies of freezing, such as the plots in Figure 2, proved to be highly reproducible. The different melting characteristics of the PPP and cocoa butter were as expected, with a sharp peak for the former, relatively pure, component, and a broad, almost bimodal distribution for the latter due to the mixture of TG, the presence of other minor components, and the possible formation of various polymorphs (11). The tail in the cocoa butter was still evident at –15°C, and there is a significant peak between 2 and 15°C, which gives rise to the softness of this material and poses challenges in handling frozen droplets at room temperature. The enthalpy of solidifi-

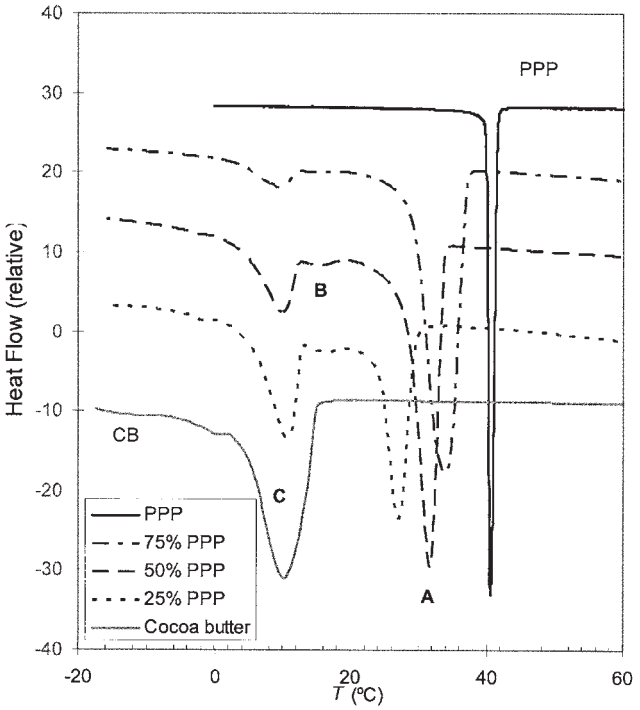

FIG. 2. DSC cooling profiles for cocoa butter (CB), tripalmitin (PPP), and their mixtures at 20 K min^{-1}.

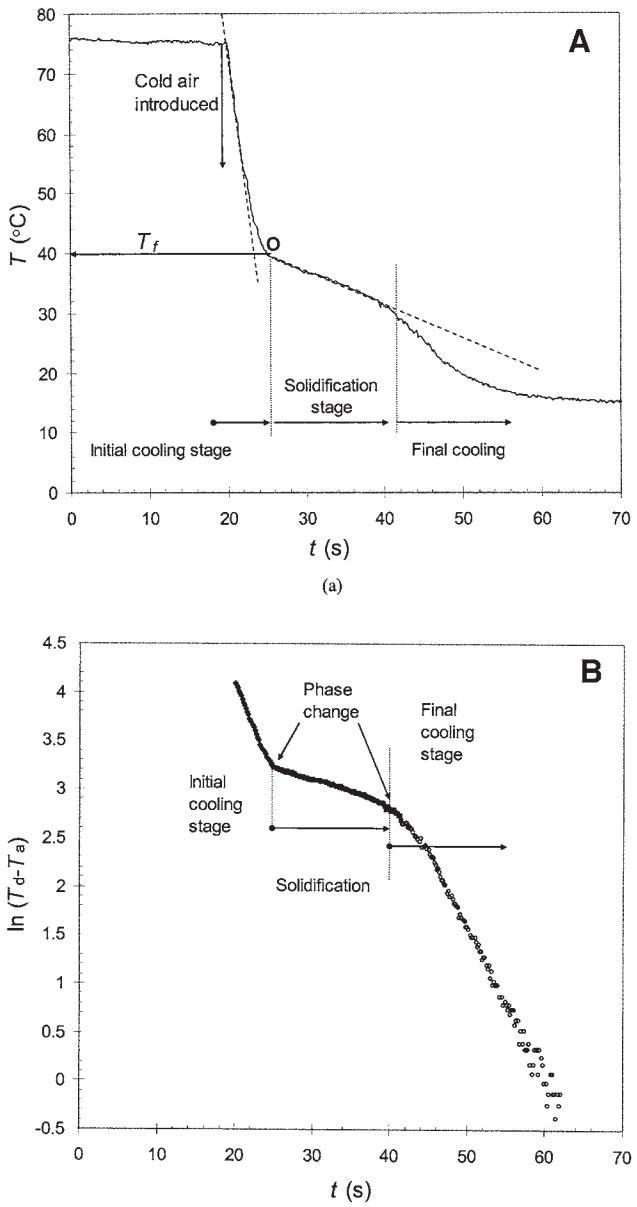

FIG. 3. Freezing a 2 mm PPP droplet at superficial velocity of u_m = 0.42 m s^{-1} and cooling air temperature of T_a = 15°C. (A) Temperature profile: dashed lines represent initial cooling and solidification cooling rates. Point O marks the onset of crystallization (phase change). (B) Data replotted in the form of the single droplet cooling model, Equation 2. For abbreviation see Figure 2.

cation for PPP, 120 J g^{-1}, compares favorably with that of 127 J g^{-1} reported for the α form of the pure component by Hagemann and Rothfus (12). The onset temperature of solidification, at 38.8°C, is significantly lower than the temperatures reported for the melting of higher-purity PPP polymorphs, namely, 46ºC (α), 49.5ºC (β′), and 63ºC (β) obtained with a 99% purity material by Fitzgerald (13) using the same device.

The cooling profiles for the mixtures show three characteristic peaks, labeled A–C (Fig. 2). Peak A is attributed to the crystallization of a PPP-rich phase from the fat mixture, with the onset temperature decreasing with decreasing PPP content. A simple model based on treating the solution as an ideal mixture did not predict the change in this parameter well, indicating that heats of mixing are significant. Peak C corresponds to the main peak in cocoa butter, and its onset and peak temperature do not change markedly with composition, whereas peak B is a transition not observed in cocoa butter, possibly the result of cocrystallization of PPP and some constituent of the cocoa butter (e.g., 1,3-dipalmitoyl-2-oleoyl glycerol). A similar feature to Peak B was observed using DSC by Cebula and Smith (14), who cocrystallized a mixture of PPP-rich fat and cocoa butter. These DSC studies thus suggest that freezing of these solutions will feature crystallization of a PPP-rich phase followed by solidification of a modified cocoa butter matrix. It should be noted that the cooling rates used in the DSC, on the order of 20 K min^{-1}, are an order of magnitude smaller than those typical of the droplet freezing studies.

Freezing behavior: droplets. Figure 3A shows a typical temperature profile for freezing of a single droplet of PPP in air at 15°C. Initial cooling at ~10 K s^{-1} is interrupted at point O by the onset of solidification of PPP at T_f (the freezing point), which was observed to lie between 39 and 41°C and was insensitive to air flow rate and temperature (with T_a below 20°C). The range of cooling rates observed is recorded in Table 1. There is an increase in cooling rate after the droplet temperature reaches ~32°C, corresponding to the end of the phase transition in Figure 2, indicating that the droplet has been mostly solidified at this point and the rate of (sensible) cooling starts to increase. The reasonably close correlation to the DSC data is noteworthy. There is only a very small amount of supercooling (0–3°C) relative to the DSC data and an absence of subsequent

TABLE 1
Freezing Parameters

Material	u_m (m s^{-1})	T_a (°C)	Initial cooling rate (K s^{-1})	Initial solidification cooling rate (K s^{-1})	h_o (W m^2 K^{-1})	*Nu*	*Nu* calculated[a]
Tripalmitin	0.42	13–15	8.5–12.5	0.5–0.6	125–150	12–14	8
	0.83	14–16	10–14	0.6–1	150–160	11–16	11
Cocoa butter	0.42	2–5	13–17	0.2–0.4	93–95	7–8	7–8
	0.83	2–6	7–9	0.5	110–135	9–11	10

[a]Calculation described in Reference 9.

recalescence as is observed in water and solutions of sucrose and coffee (9), all of which feature significantly more supercooling before nucleation compared with the fat systems considered here. With pure liquids the temperature remains near T_f after recalescence until the droplet is completely frozen, whereas the linear decrease in freezing temperature with time evident in the figure may be due to heat transfer or freeze concentration owing to the impurities in the PPP.

The phase transitions are very apparent when the data are plotted against the simple freezing model presented in Reference 9:

$$\frac{\pi d^3}{6}\rho C_p \frac{dT_d}{dt} = \pi d^2 h_o (T_d - T_a) \quad [1]$$

where d = droplet diameter, ρ = density, C_p = specific heat capacity, t = time, and h_o = surface film heat transfer coefficient. Equation 1 yields the temperature profile

$$\ln(T_d - T_a) = \frac{6h_o t}{C_p \rho d} \quad [2]$$

This will exhibit discontinuities at phase transitions where the apparent heat capacity, C_p, changes. Figure 3B shows the data replotted in this form; the phase transitions are immediately apparent.

The components in cocoa butter freeze over a wider range of temperatures, and the cooling profile in Figure 4 shows a sharp change in cooling rate at a T_f value of 15 ± 1°C (confirmed by plotting the data in the form of Eq. 2) but no later change associated with completion of freezing and cooling of the solidified droplet. This behavior is consistent with the data in Figure 2A: The DSC freezing peak features a long tail, suggesting solidification is not complete at T_a = 4°C.

Equation 2 also allows the surface heat transfer coefficient, h_o, to be estimated, and the values of the corresponding Nusselt number ($Nu = h_o d/l$) are compared in Table 1 with those estimated using the Ranz and Marshall correlation (15): The agreement is particularly good for the cocoa butter.

Figure 5 shows the cooling profiles for the three mixtures studied: All exhibit rapid initial cooling, and three parts in the freezing stage marked by changes in slope in the heat transfer model (Eq. 2) plot (illustrated by the inset in the 50:50 profile). The temperatures of the transitions are marked on the Figure as $T_{f,\mathrm{PPP}}$, $T_{f,\mathrm{mixture}}$, and $T_{f,\mathrm{cocoabutter}}$. The $T_{f,\mathrm{PPP}}$ value decreases significantly with PPP content, i.e., 38, 33, and 28°C for 75, 50, and 25 wt% of PPP, respectively, corresponding extremely well to the corresponding DSC data (37, 33, and 30°C, respectively). The values of $T_{f,\mathrm{mixture}}$ declined more gradually from 25 to 20°C as the PPP content was decreased from 75 to 25 wt%. There was no systematic variation with PPP content for $T_{f,\ \mathrm{cocoabutter}}$, which ranged from 11 to 15°C. The values of $T_{f,\mathrm{mixture}}$ and $T_{f,\mathrm{cocoabutter}}$ corresponded reasonably closely to the DSC traces (17 and 11°C, respectively), which showed minimal variation with composition. The discrepancy in $T_{f,\mathrm{mixture}}$ may be due to the difference in cooling rates or the true temperature profile in the droplet. These results are consistent with PPP crystallizing preferentially from the melt, followed by freezing of the fat mixture: This aspect requires further investigation.

Microstructure: SEM and CSEM. The SEM images of the surface of frozen PPP droplets in Figure 6 show that the structure can undergo recrystallization over time. Droplets were generated under similar conditions [u_m = 0.42 m s^{-1}: T_a = 10°C (0°C for the cocoa butter and mixtures)]: (i) stored overnight at room temperature and also imaged at room temperature, (ii) stored at 0°C and imaged at –150°C. Both images showed sur-

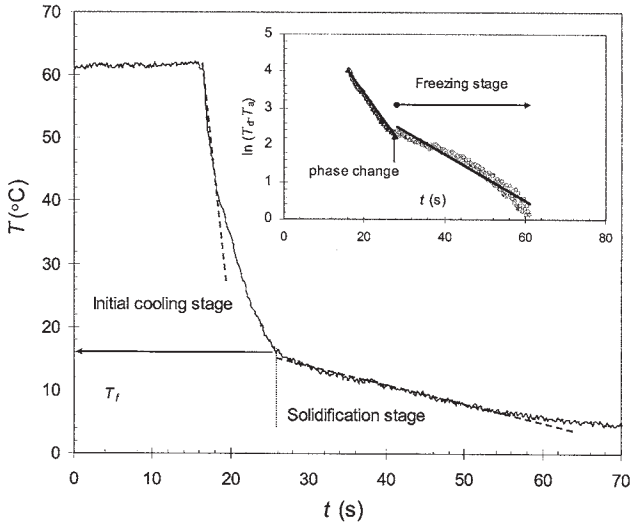

FIG. 4. Typical temperature profile of freezing a cocoa butter droplet at u_m = 0.42 m s^{-1} and T_a = 4°C. Dashed lines denote initial cooling and solidification cooling rates. Inset shows data plotted in form of Equation 2. For abbreviations see Figures 1 and 3.

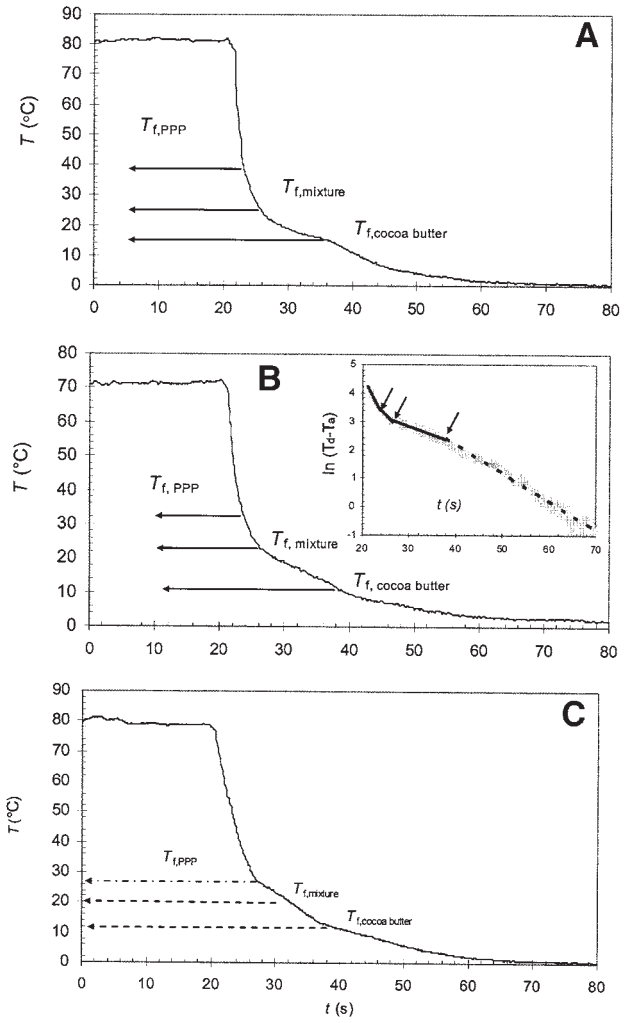

FIG. 5. Temperature profiles of single droplet freezing for PPP/CB mixtures. (A) 25:75; (B) 50:50, inset shows freezing model construction; (C); 75:25 wt%. u_m = 0.42 m s^{-1}, T_a ~ 0°C. For abbreviations see Figures 2 and 3.

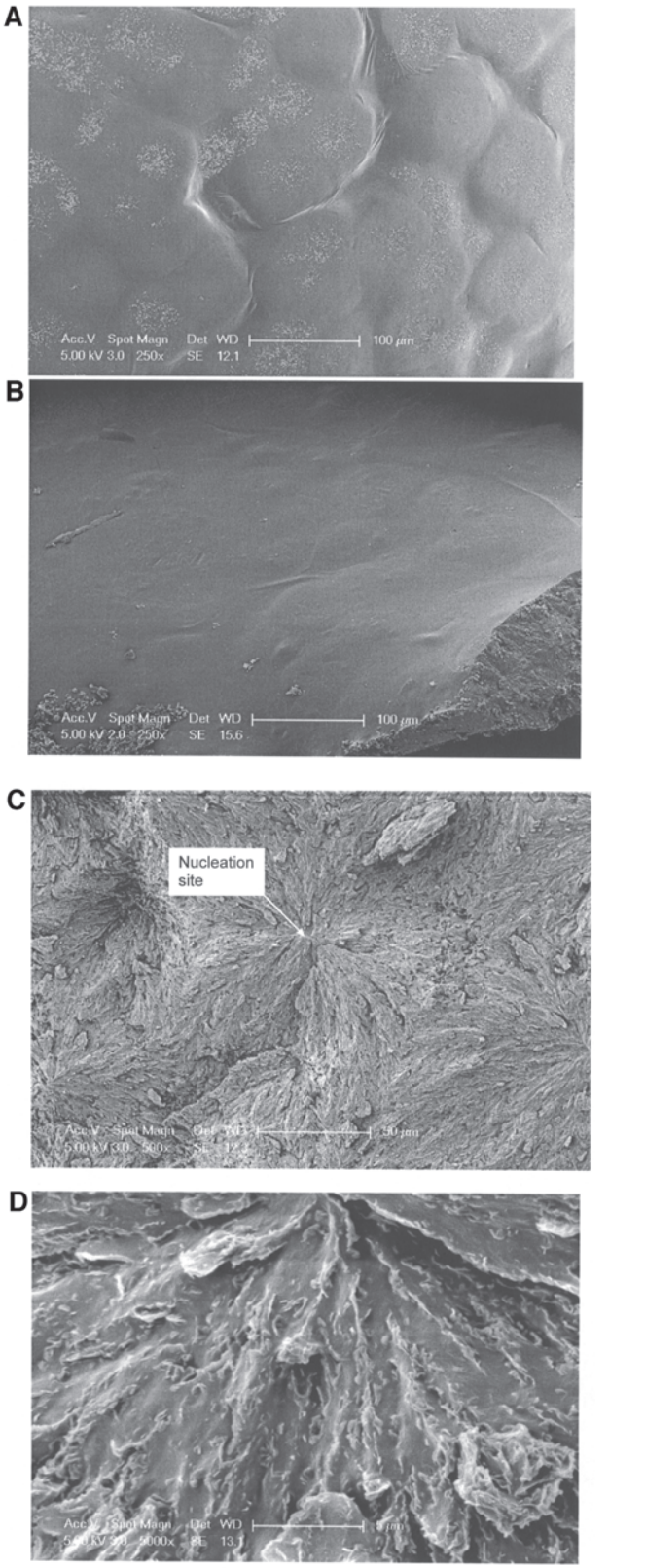

FIG. 6. Scanning electron micrograph (SEM) images of frozen PPP droplets. (A) Outer surface, stored and imaged at room temperature, 250×; (B) outer surface, stored at 0°C and imaged at –150°C, 250×; internal microstructure of droplet in (B) at (C) 500×; (D) 5000×. For abbreviation see Figure 2.

faces characterized by small plates (dimension ± 100 micron), which were much more evident in the droplet stored at room temperature. The bright spots on Figure 6A proved to be shards, confirming that recrystallization was occurring. Storage method did not affect the internal microstructure with a homogeneous flower-like structure around distinct nucleation points (Figs. 6C, 6D).

The image in Figure 7A of frozen cocoa butter droplets stored at room temperature after solidification again shows that small platelets were evident on the surface: Such platelets were not evident on those stored at 0°C (Fig. 7B). Rapid cooling of the cocoa butter melt is likely to form the type I polymorph (Table 2) on the surface, which melts at 17.3°C and can transform to the Type II form, which has a m.p. at 23.3°C (Table 2). The inner microstructure of the droplets in Figure 7C shows a uniform and fine crystal structure but with none of the nucleation site features evident in PPP (Fig. 6C).

The internal microstructure of mixtures of PPP and cocoa

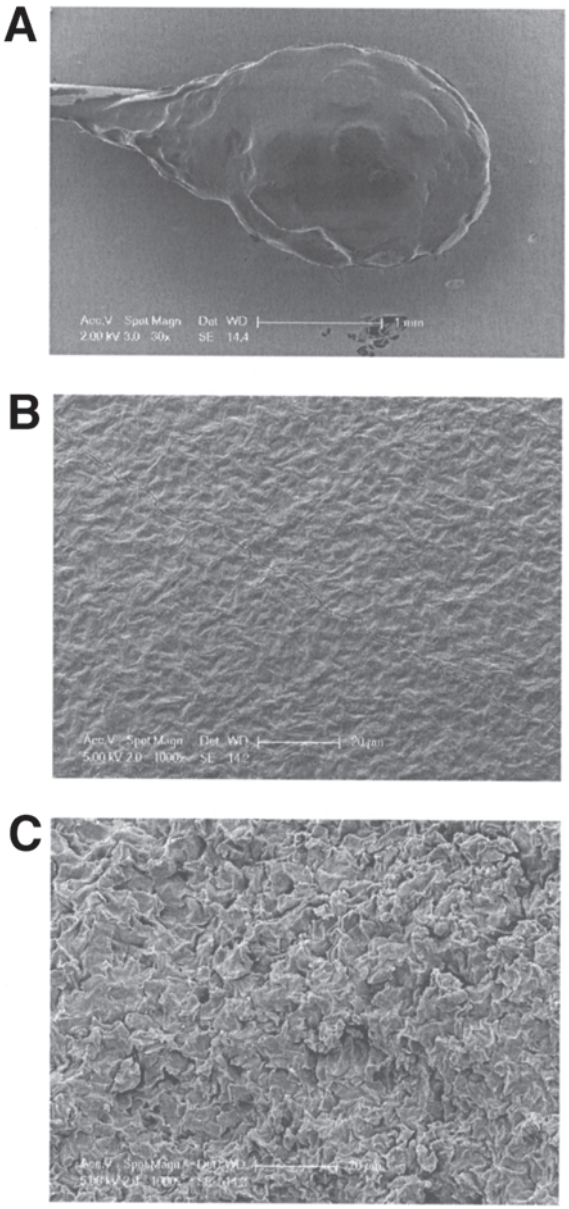

FIG. 7. SEM images of frozen CB droplets. (A) Outer surface, stored and imaged at room temperature, 30×; (B) outer surface, stored at 0°C and imaged at –150°C, 1000×; (C) internal microstructure of droplet in (B), 1000×. For abbreviations see Figures 2 and 6.

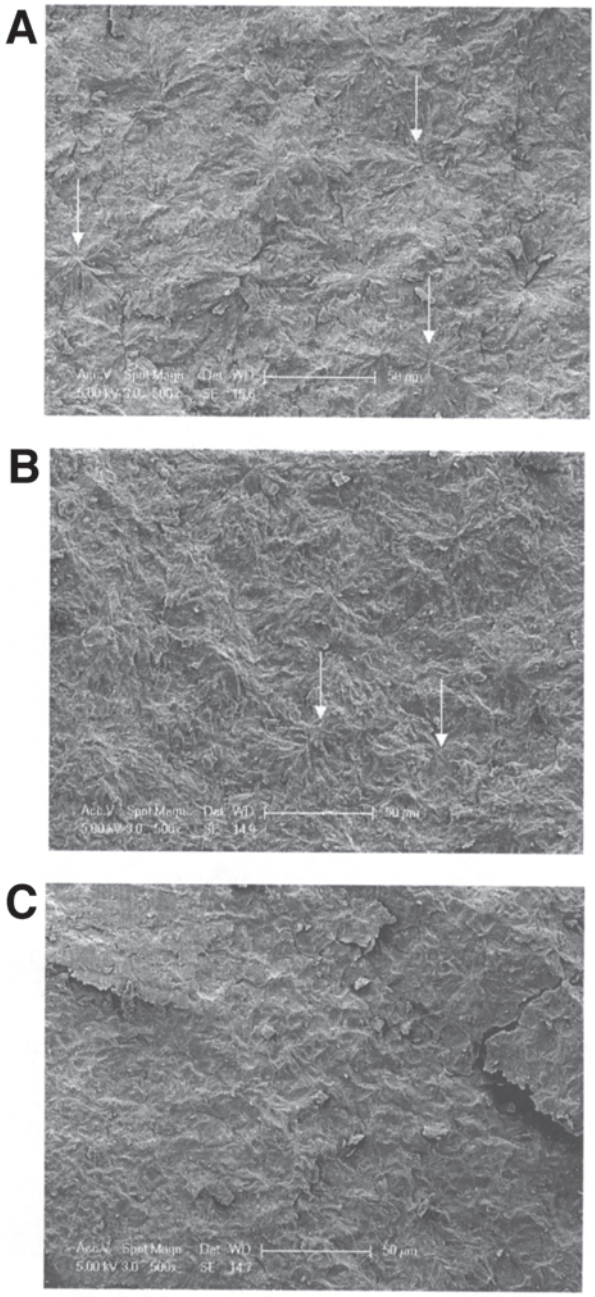

FIG. 8. Internal microstructure of frozen droplets of PPP/CB mixtures (in wt%) (A) 75:25; (B) 50:50; (C) 25:75%. (500×). Arrows indicate examples of nucleation sites. For abbreviations see Figure 2.

butter in Figure 8 all show a finely divided structure with nucleation site patterns (shown by the arrows), similar to those observed in PPP alone, becoming less prevalent as the fraction of PPP decreases.

Electron microscopy therefore demonstrated that the surface microstructures achieved are sensitive to temperature variation after formation, whereas the bulk structure is relatively insensitive to such factors.

XRD. XRD was used to identify the polymorphic forms present in the solidified droplet bulk. All droplets analyzed by XRD were generated on nail-varnish-coated glass filaments at u_m = 0.42 m s^{-1} and T_a = –12°C and were stored at 0°C before testing later that day. The raw XRD patterns and integrated intensity profiles are shown in Figures 9 and 10, respectively. The former plots showed that the crystal structures were isotropic, with no preferential orientation. PPP appeared to be characterized by a single strong peak at small angles and three small, but well-defined, peaks at large angles. A weak peak was observed at 6.7°. Cocoa butter exhibited three weak peaks in the SAXS region (either side of the PPP peak) and five small, noisy peaks at larger angles: Cocoa butter and PPP share a very strong peak at approximately 19°. Wide-angle spectra were also collected for cocoa

TABLE 2
Polymorphism in Cocoa Butter Under Quiescent Conditions Reported by Sonwai (17)

Polymorph	M.p. (°C)	Conditions
Form I (γ)	17.3	Rapid cooling of melt
Form II (α)	23.3	Cooling of melt at 2 K min^{-1} Rapid cooling of melt followed by storing for several minutes up to 1 h at 0°C
Form III (β'_2-2)	25.5	Solidification of melt at 5–10°C. Transformation of form II by storing at 5–10°C
Form IV (β'_1-2)	27.5	Solidification of melt at 16–21°C Transformation of form III by storing at 16–21°C
Form V (β_2-3)	33.8	Solidification of melt, transformation of form IV, or solvent crystallization
Form VI (β_1-3)	36.3	Transformation of form V (4 mon at room temperature)

butter and PPP at angles greater than 25.5°, but no additional peaks were observed for either substance or their mixtures.

Table 3 is a summary of the peaks observed in this study compared with those reported in the literature. The combined WAXS/SAXS data between 2 θ = 2.2–26° for PPP compared extremely well with the spectrum for the β polymorph in the International Centre for Diffraction Data (ICDD) Powder Diffraction File (ICDD PDF# 30-1994, http://www.icdd.com). Differences in cocoa butter at source mean that reference spectra for each polymorph, particularly Forms V and VI, are not readily available (16), so the cocoa butter spectra generated here were compared with the classification reported by Sonwai (17), based on crystallization of a cocoa butter under quiescent conditions (Tables 2, 3). It should be noted that the XRD data will be dominated by structure in the bulk of the droplet: Other forms may be present at the surface but will not contribute significantly to this form of inspection.

The spectra in Figure 10 and analysis in Table 3 suggest that the solidified droplets consisted of CB Forms V and/or VI, which share several similar peaks. The similarity of diffraction peaks for Forms V and VI has been discussed by van Malssen *et al.* (19) and Loisel *et al.* (20): both exhibit distinct strong peaks in the SAXS region at ~1.35 and ~2.75°, with Form VI showing a faint peak at 2.0° (20). This peak was difficult to detect with SAXS/air but was evident with SAXS/He (data not shown). In the WAXS region, the cocoa butter exhibits four small peaks that distinguish it from PPP but that complicate identification of the polymorph. Forms V and VI have four and three peaks, respectively, in this 2 θ range; they are, however, relatively weak and only appear distinctly in high-quality diffractograms. Nevertheless, the likelihood of the spectra originating from other polymorphs is small.

Figure 10 shows that the peaks observed in the mixtures are found at the same angles as peaks in the individual substances, indicating that the components both crystallize in the more sta-

TABLE 3
Peaks[a] Located in X-Ray Diffraction of Cocoa Butter (CB), Tripalmitin (PPP) Mixtures

Peak	Origin	Reference	PPP	Observed mixtures	CB
0.75	PPP		w	—	—
1.35°	CB	19	—	w (some)	1°, 1.55°, m
2.0°	CB	20	—	—	SAXS/He, w
2.2°	PPP	ICDD	s	m	—
2.75°	CB	19	—	—	2.7–3°, m
6.6°	PPP	ICDD	m	w	—
16.5°	PPP	ICDD	w	—	w
17.2°	PPP	ICDD	w	—	—
19°–	PPP	ICDD	s (19.5°)	s	s
19.5°	CB V and VI	17	—	—	—
22°	CB VI	17	—	—	—
22.3°	CB V	17	—	—	m
23.0°	CB VI	17	—	—	w
23.2°			m	m-w	—
23.7°	CB V	17	—	—	m
24.05°	CB VI	17	—	—	w
24.1	PPP	ICDD	m	m-w	—
24.5°	—	—	—	—	w

[a] s, strong; m, medium; w, weak.

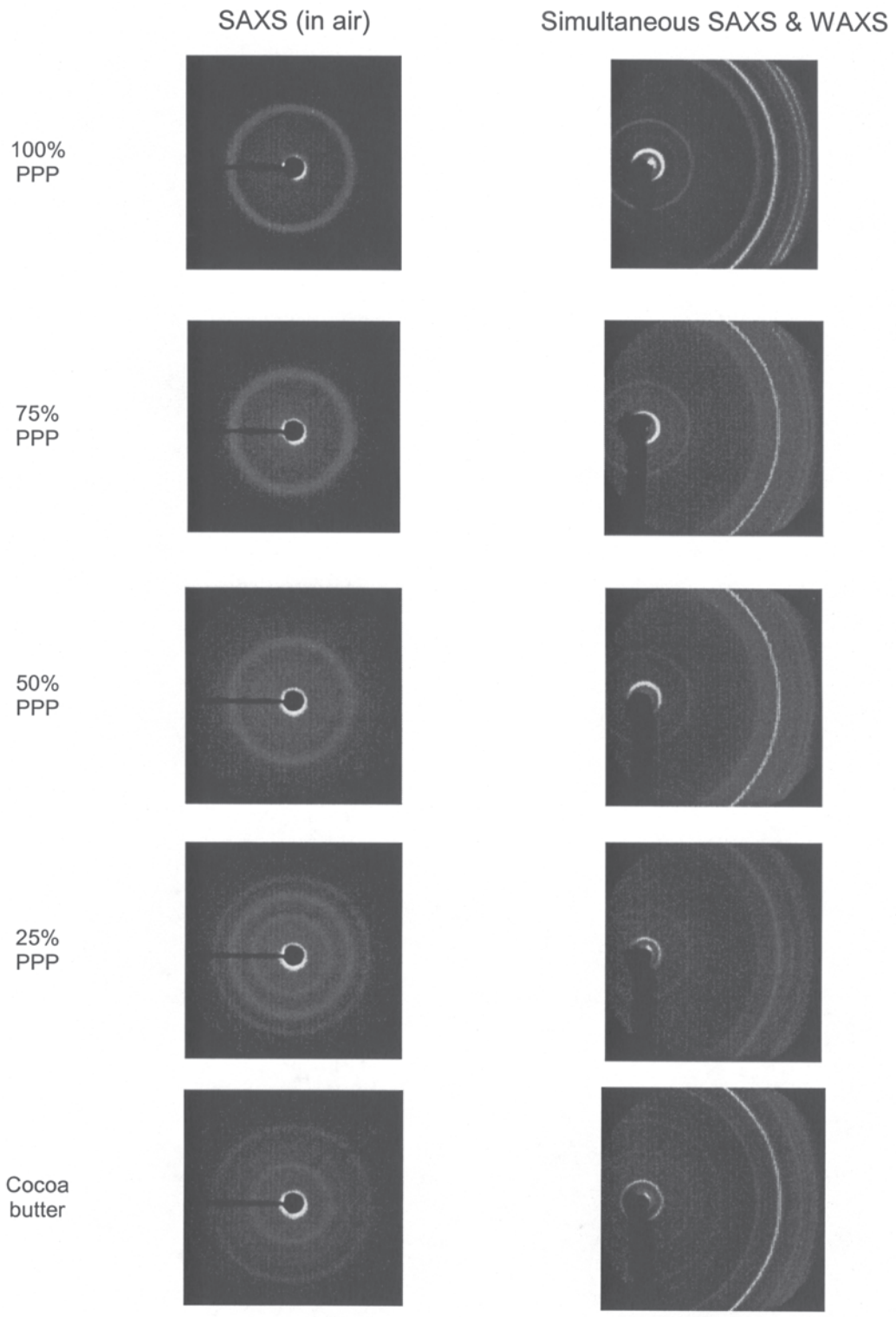

FIG. 9. Diffraction patterns of solidified droplets. SAXS, small-angle scattering; WAXS, wide-angle scattering. For other abbreviation see Figure 2.

ble β and V/VI Forms. These forms are highly unlikely to have formed during initial crystallization and freezing of the droplets, as evidenced by the general agreement of the freezing apparatus data with that provided by the DSC, which supported the formation of less stable polymorphs for both cocoa butter and PPP. Following solidification, the droplets were immediately transferred from the freezing apparatus to a cold chamber (temperature below 0°C) for transportation to the X-ray equip-

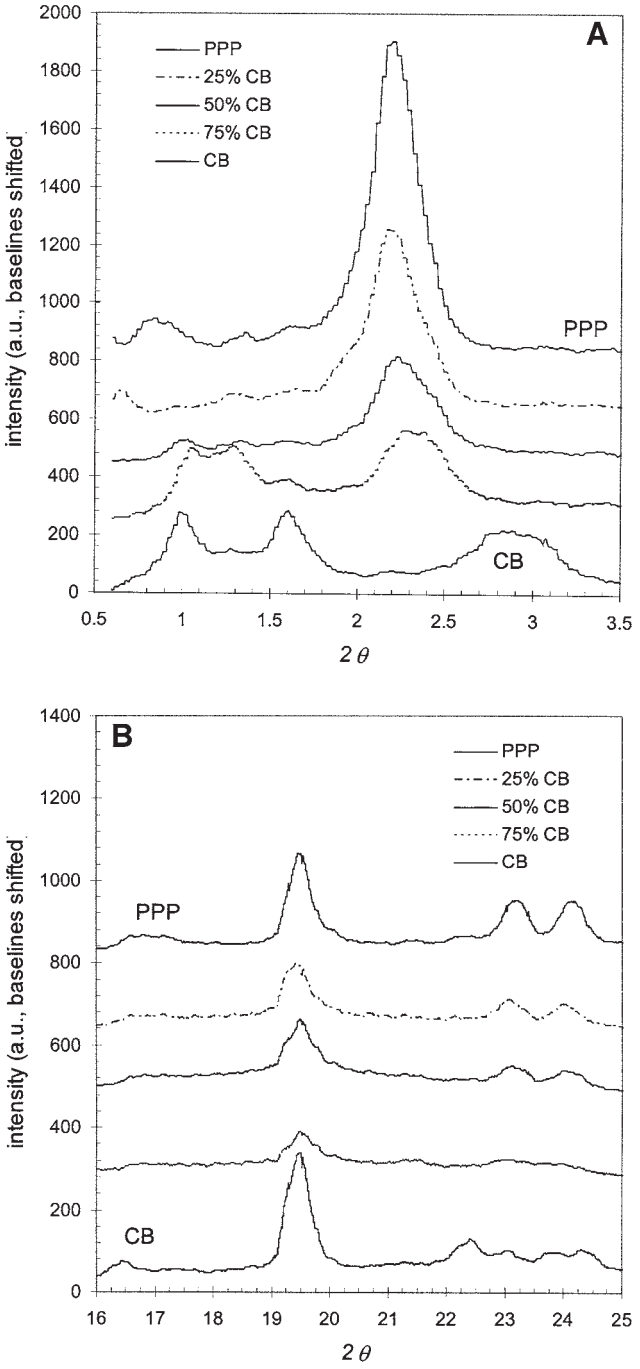

FIG. 10. Diffraction spectra for frozen droplets: (A) SAXS in air ($0.8° < 2\theta \leq 3.3°$) and (B) WAXS ($16° < 2\theta \leq 25.5°$). For abbreviations see Figures 2 and 9.

ment. A maximum of 5 min was required for sample preparation and data acquisition. Based on a consideration of heat transfer to the droplets from stagnant air, this is just sufficient time for the droplet to reach ambient temperature. Thus, recrystallization into the more stable forms is extremely rapid. The effect of reducing the fraction of PPP in Figure 10B is to reduce the intensity and definition of the PPP peaks: Only with the smallest fraction (25 wt% PPP) do the cocoa butter peaks appear. The intensity of the PPP peak is approximately proportional to the amount of PPP present, which is consistent with the crystallization of PPP alone followed by solidification of a fat matrix. Further work will also focus on linking this behavior to the phase diagram of these mixtures.

ACKNOWLEDGMENTS

Funding RJG from an IChemE Pharma Subject Group Bursary and for DTC from EPSRC is gratefully acknowledged. Several items of apparatus used in this project were funded by the Food Processing Faraday Fast Track Scheme. We wish to thank the following colleagues for assistance with testing and helpful discussions: Tony Burgess (BioImaging Centre—SEM analysis); Zlatko Saracevic and Reilly Nigo (Chemical Engineering—DSC analysis).

REFERENCES

1. Meryman, H.T., Sublimation Freeze Drying Without a Vacuum, *Science 130*:628–629 (1959).
2. Mumenthaler, M., and H. Leuenberger, Atmospheric Spray-Freeze Drying: A Suitable Alternative in Freeze Drying Technology, *Intl. J. Pharm. 72*:97–110 (1991).
3. Windhab, E., New Developments in Crystallization Processing, *J. Thermal Anal. Calorim. 57*: 171–180 (1999).
4. Brooker, B.E., Method and Apparatus for Very Low Temperature Processing, Japanese Patent JP2002291407 (2002).
5. Brooker, B.E., and R.I. Tomlins, Cryogenic Crystallization of Fats, European Patent EP1285584 (2003).
6. Brooker, B.E., and R.I. Tomlins, Manufacture of Ice Cream, European Patent EP1530426 (2005).
7. Hindmarsh, J.P., A.B. Russell, and X.D. Chen, Experimental and Numerical Analysis of the Temperature Transition of a Freezing Food Solution Droplet, *Chem. Eng. Sci*., *59*:2503–2515 (2004).
8. Hindmarsh, J.P., K.G. Hollingsworth, D.I. Wilson, and M.L. Johns, An NMR Study of Freezing of Emulsion-Containing Drops, *J. Colloid Interface Sci. 275*:165–171 (2004).
9. MacLeod, C.S., J.A. McKittrick, J.P. Hindmarsh, M.L. Johns, and D.I. Wilson, Fundamentals of Spray Freezing of Instant Coffee, *J. Food Eng. 74*:451–461 (2006).
10. Lutton, E.S., Lipid Structures, *J. Am. Oil Chem. Soc. 49*, 1–9 (1972).
11. Davis, T.R., and P.S. Dimick, P.S. Isolation and Thermal Characterization of High-Melting Seed Crystals Formed During Cocoa Butter Solidification, *Ibid. 66*:1488–1493 (1989).
12. Hagemann, J.W., and J.A. Rothfus, Computer Modeling of Monoacid Triglyceride α-Forms in Various Subcell Arrangements, *Ibid. 60*:1123–1131 (1983).
13. Fitzgerald, A.M., Crystallisation and Deposition Behaviour of Palm Oil Fractions, Ph.D. Dissertation, University of Cambridge, Cambridge, United Kingdom (2002).
14. Cebula, D.J., and K.W. Smith, Differential Scanning Calorimetry of Confectionary Fats. 2. Effects of Blends and Minor Components, *J. Am. Oil Chem. Soc. 69*, 992–998 (1992).
15. Ranz, W.E., and W.R. Marshall, Jr., Evaporation from Drops. Parts 1&2, *Chem. Eng. Prog. 48*:141–146, 173–180 (1952).
16. van Langevelde, A., K. van Malssen, R. Peschar, and H. Shenk, Effect of Temperature on Recrystallization Behavior of Cocoa Butter, *J. Am. Oil Chem. Soc. 78*:919–925 (2001).

17. Sonwai, S. The Effect of Shear on the Crystallisation of Cocoa Butter, Ph.D. Dissertation, University of Cambridge, Cambridge, United Kingdom (2003).
18. Schlichter-Aronhime, J., and N. Garti, Reconsideration of Polymorphic Transformations in Cocoa Butter Using the DSC, *J. Am. Oil Chem. Soc. 65*:1140–1143 (1988).
19. van Malssen, K., A. van Langevelde, R. Peschar, and H. Schenk, Phase Behavior and Extended Phase Scheme of Static Cocoa Butter Investigated with Real-Time X-Ray Powder Diffraction, *Ibid. 76*:669–676 (1999).
20. Loisel, C., G. Keller, G. Lecq, G. Bourgaux, and M. Ollivon, Phase Transitions and Polymorphism of Cocoa Butter, *J. Am. Oil Chem. Soc. 75*:425–439 (1998).

[Received October 6, 2005; accepted August 30, 2006]